Dalton Transactions

COMMUNICATION

View Article Online
View Journal | View Issue

Cite this: *Dalton Trans.*, 2015, **44**, 13469

Received 20th January 2015,
Accepted 25th June 2015

DOI: 10.1039/c5dt00262a

www.rsc.org/dalton

A CO_3^{2-}-containing, dimanganese-substituted silicotungstate trimer, $K_9[H_{14}\{SiW_{10}Mn^{II}Mn^{III}O_{38}\}_3(CO_3)]\cdot 39H_2O$†

Ling Yang, Qisen Liu, Pengtao Ma, Jingyang Niu* and Jingping Wang*

An unprecedented silicotungstate trimer $K_9[H_{14}\{SiW_{10}Mn^{II}Mn^{III}O_{38}\}_3(CO_3)]\cdot 39H_2O$ (1) has been successfully synthesized, in which the CO_3^{2-} resides inside the three Keggin $\{SiW_{10}Mn^{II}Mn^{III}O_{38}\}$ units and the three O atoms serve as μ_2-O atoms to connect with three Mn^{III}. Magnetic investigation indicates that 1 exhibits antiferromagnetic coupling.

Rational design, synthesis and investigation of properties of polynuclear transition-metal compounds are of great current interest, largely driven by their structural diversity and potential applications.[1] What is most notable in this field is the research on transition-metal-substituted POMs (TMSPs), many of which possess aesthetically pleasing structures and, more importantly, fascinating magnetic properties resulting from the strong intramolecular exchange interactions among the paramagnetic metal clusters and the negligibly weak intermolecular exchange interactions between POM clusters.[2] This unique phenomenon can be attributed to the existence of diamagnetic POM ligands, which are a large class of highly modifiable, discrete metal–oxygen anionic clusters with versatile sizes and can act as unique inorganic multidentate O-donor ligands to trap more metal centers forming giant aggregates. For example, many high-nuclearity, Mn-containing POMs have been obtained,[2a,3] which are largely stimulated by the multiple valence of manganese and a large uniaxial anisotropy derived from the presence of the Jahn–Teller distorted Mn^{III} ions.[2a,4] In this stage, manganese-substituted silicotungstates largely expand the field of POM chemistry. However, a majority of reported compounds are monomeric or sandwich-type POMs, and the trimeric or giant POMs are rare (a detailed survey of manganese-substituted silicotungstate derivatives is provided in the ESI, Table S1†). Therefore, the assembly of Mn-substituted trimeric silicotungstate[5] or any other POM subfamily still remains a significant synthetic challenge. A major reason is the relatively inherent connection mode between lacunary silicotungstates and manganese ions. Considering that the facilitating ligand CO_3^{2-} may tune the coordination mode between the POM and the metal ions and with the fact that CO_3^{2-} can be encapsulated by a metal cluster,[6] we decided to continue to explore and synthesize novel silicotungstate derivatives with K_2CO_3 by adjusting the pH. It is exciting that we obtained one CO_3^{2-}-containing, dimanganese-substituted silicotungstate trimer, $[\{SiW_{10}Mn^{II}Mn^{III}O_{38}\}_3(CO_3)]^{23-}$ (**1a**). To our knowledge, this trimeric structure has never been reported before, and polyoxoanion **1a** displays a 3-fold rotational axis consistent with C_3 symmetry.

Deep-brown block crystals of **1** were obtained by the reaction of $K_6Na_2SiW_{11}O_{39}\cdot 13H_2O$[7] precursor and $[Mn_{12}O_2(OMe)_2(thme)_4(OAc)_{10}(H_2O)_4]\cdot 2MeOH$[8] (abbreviated as $\{Mn_{12}\}$) by slowly adjusting the pH to *ca.* 10.0 with 2.0 mol L^{-1} K_2CO_3 under conventional solution conditions. Given that the CO_3^{2-} was introduced into the cavity of trimeric silicotungstate, we surmised that the CO_3^{2-} not only can adjust the pH value of the system but also can change the inherent mode of connections between POM and manganese ions. Moreover, the experimental powder X-ray diffraction (XRPD) pattern for **1** is in good agreement with the simulated XRPD pattern from the single-crystal X-ray diffraction, demonstrating good phase purity for **1** (Fig. S1 in the ESI†).

Single-crystal X-ray structural analysis reveals that **1** is crystallized in the hexagonal space group *R3m*. The molecular structure of **1** is made up of a cyclic trimeric $[\{SiW_{10}Mn^{II}Mn^{III}O_{38}\}_3(CO_3)]^{23-}$ polyoxoanion (Fig. 1a), 9 potassium cations, 14 hydrogen cations for charge balance, and 39 lattice water molecules.‡ All the Mn centers encapsulated by lacunary POM ligands have four coordination bonds to the polytungstate unit. **1a** can be described as a clover-leaf structure with the CO_3^{2-} lying in the center from the top view of the

Key Laboratory of Polyoxometalate Chemistry of Henan Province, Institute of Molecular and Crystal Engineering, College of Chemistry and Chemical Engineering, Henan University, Kaifeng 475004, China. E-mail: jyniu@henu.edu.cn, jpwang@henu.edu.cn; Fax: (+86) 371-23886876

†Electronic supplementary information (ESI) available: The experiment sections of **1**. The comprehensive literature survey of manganese-substituted silicotungstate derivatives. The actual and thumbnail array polyoxoanion structure of **1**, XRPD spectra, XPS spectra, bond valence sum calculations, IR spectra, CVs, TG analyses, UV-vis spectra and other electronic formats. See DOI: 10.1039/c5dt00262a

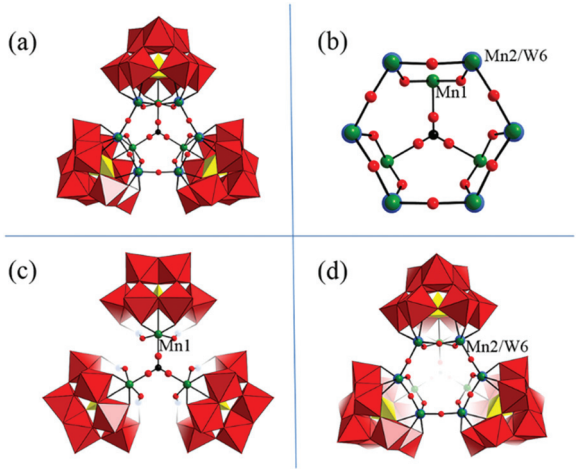

Fig. 1 (a) Polyhedral/ball-and-stick representation of $[\{SiW_{10}Mn^{II}Mn^{III}O_{38}\}_3(CO_3)]^{23-}$, (b) isolated core unit of **1a**. (c) The second layer of $[\{SiW_{10}Mn^{II}Mn^{III}O_{38}\}_3(CO_3)]^{23-}$, (d) the first layer of $[\{SiW_{10}Mn^{II}Mn^{III}O_{38}\}_3(CO_3)]^{23-}$. All solvent water molecules and cations are omitted for clarity. Color code: light blue spheres: W; green spheres: Mn; yellow tetrahedral: Si; black spheres C; red polyhedra: WO_6.

structure. Alternatively, **1a** can also be seen as a "double-layer" structure. The first layer can be described as three Mn^{II}/Mn^{III} di-substituted Keggin $[SiW_{10}Mn^{II}Mn^{III}O_{38}]^{7-}$ units linked by three {Mn2–O–W6} linkages, where the manganese and tungsten atoms are statistically disordered with half occupancy for the Mn2 and W6 positions (Fig. 1d). This phenomenon has been reported in the previous literature.[5,9] The second layer can be viewed as the assembly of a central CO_3^{2-} core which is capped by three Mn1 ions derived from the three Keggin $[SiW_{10}Mn^{II}Mn^{III}O_{38}]^{7-}$ units (Fig. 1c). The above two layers are fused together forming a "bowl shaped" core (Fig. 1b). It is necessary to point out that the three O atoms of CO_3^{2-} are disordered (Fig. S2 in the ESI†). Furthermore, the angles of Mn2–O–W6 between adjacent Keggin units are 146.7°, being larger than the Mn–O–W (134–136°) angles in $[(Mn_2^{II}GeW_{10}O_{38})_3]^{18-}$ (ref. 9*a*) and the Mn–O–W angles (145°) in $[(\beta_2\text{-}SiW_{11}MnO_{38}OH)_3]^{15-}$,[5] a significant reason of which may be attributed to the influence of CO_3^{2-}. In addition, the **1a** subunits are linked by potassium cations to generate the 3D architecture.

An attractive characteristic in **1** is that the inorganic bridging role of the CO_3^{2-} lying inside the center of three Mn1 is unusual in POM chemistry while there are several reported compounds in which the CO_3^{2-} participates in the coordination. In $K_8Na_{10}[Mn_2^{IV}Mn_6^{III}Mn_4^{II}(\mu_3\text{-}O)_6(\mu\text{-}OH)_4(H_2O)_2(CO_3)_6][B\text{-}\beta\text{-}SiW_6O_{26}]_2{\cdot}30H_2O$,[2a] the six CO_3^{2-} have the same coordination environment, that is there are two O atoms that act as μ_2-O atoms and coordinate to Mn^{III} and Mn^{IV} respectively and the third O atom acts as the terminal atom. In $K_6[W_4O_8(O_2)_6(CO_3)]{\cdot}6H_2O$,[10] two μ_2-O atoms coordinate to the W atom and the other O atom as the terminal atom. In **1a**, all three O atoms of CO_3^{2-} serve as μ_2-O atoms to connect with three Mn^{III}. Another noteworthy feature of polyoxoanion **1a** is that the three $Mn^{III}1$ cations display a distorted octahedral geometry with one atom derived from the CO_3^{2-} and five atoms from the polyoxoanions. Moreover, the previous literature shows that the cavity of similar trimeric silicotungstates is usually occupied by nothing.[5,11] The cavity of similar trimeric tungstogermanates is usually occupied by counter-cations,[9a] transition metals.[9b] So, it is inspiring that the CO_3^{2-} was introduced into the cavity of trimeric silicotungstate.

According to the charge balance consideration and bond-valence sum calculations (BVS) analyses,[12] all the Mn1 and W atoms are in the +3 and +6 oxidation states, respectively, and this result is further confirmed by X-ray photoelectron spectra (XPS) measurement. The existence of Mn^{3+} ions can also be further testified by the crystal colour of **1** and UV-vis spectroscopy (Fig. S3 in the ESI†). The absorption band at 472 nm in the visible region results from the d–d electron transition of Mn^{III} centers. Moreover, the oxidation states of all Mn2 centers are +2, which are determined by means of XPS instead of BVS because of the disorder between Mn2 and W. As shown in Fig. S4a in the ESI,† the XPS spectra of **1** exhibit two strong peaks at 34.4 and 36.5 eV, attributed to $W^{6+}(4f_{5/2})$ and $W^{6+}(4f_{7/2})$, respectively.[13] In Fig. S4b in the ESI,† the Mn 2p region features a spin–orbit doublet with Mn $2p_{1/2}$ and Mn $2p_{3/2}$. Both the Mn $2p_{3/2}$ spectra and Mn $2p_{1/2}$ spectra can be divided into two characteristic peaks, and the binding energies of the Mn $2p_{2/3}$ peak are 642.2 and 640.6 eV confirming the Mn valence state as Mn^{3+} and Mn^{2+}, respectively. The Mn $2p_{3/2}$ binding energies are basically in good agreement with pure Mn_2O_3 and MnO.[14] The smaller deviation is due to the fact that the binding energy bears on the chemical environment, and the absence of the appropriate internal Mn reference peaks increases a lot of difficulties to accurately detect the chemical shift. According to the charge balance, fourteen protons should be added. In order to locate the positions of these protons, all the oxygen atoms of the POM fragments are carried out based on the BVS calculations (Fig. S5, Tables S2 and S3 in the ESI†).

Because of the presence of the Mn ions, and manganese-substituted POMs often exhibiting fascinating magnetic properties, the magnetic behavior of **1** was investigated. The temperature dependence of the magnetic susceptibility was measured in the range of 2–300 K at 1000 Oe. As shown in Fig. 2a, the experimental $\chi_M T$ product of **1** is equal to 21.652 $cm^3\ K\ mol^{-1}$ at 300 K, being slightly lower than the spin-only value (g = 2.0) of 22.125 $cm^3\ K\ mol^{-1}$ for three Mn^{III} (S = 2) ions and three Mn^{II} (S = 5/2) ions. Upon cooling, the $\chi_M T$ products continuously decrease to reach a minimum of 1.79 $cm^3\ K\ mol^{-1}$ at 2 K. This characteristic behavior indicates strong antiferromagnetic interactions among the manganese ions. The $1/\chi_M$ *versus* T plot is well fitted with the Curie–Weiss law between 300 and 52 K (Fig. 2b), resulting in a Curie constant C = 22.78 $cm^3\ K\ mol^{-1}$ and a Weiss constant θ = −16.7 K. The negative Weiss constant can also give further evidence of the presence of dominating antiferromagnetic exchange interaction within Mn centers from manganese-oxo clusters. In addition, the field dependence of the magnetization at 1.8 K

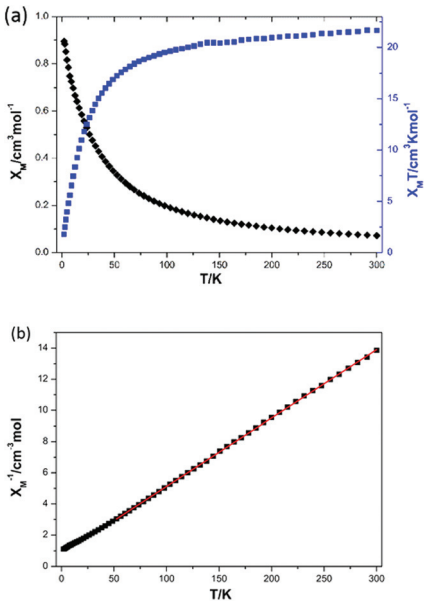

Fig. 2 (a) The temperature dependence of χ_M and $\chi_M T$ values for **1** between 2.0 and 300 K. (b) The temperature dependence of $1/\chi_M$ for **1**. The red solid line represents the best-fit by the Curie–Weiss law.

for **1** indicates that the magnetization increases continually and without the saturation state even at 70 kOe (Fig. S8 in the ESI†), which further illustrates the antiferromagnetic interactions.

The electrochemical behavior of compound **1** was studied by cyclic voltammetry (CV) (Fig. S9 in the ESI†). The redox behavior of **1** in pH 6 (1 M CH_3COONa–CH_3COOH) buffer solution shows three reduction peaks in the potential range of +1.0 to −1.0 V and the reduction peak potentials are 0.446, −0.103, and −0.948 V (*vs.* SCE), respectively. The first two reduction waves located at 0.446 and −0.103 V and one single oxidation process (0.756 V) are attributed to the redox processes of the Mn centers. The peak at −0.103 is attributed to the reduction of the Mn center of Mn^{III}, and the other redox process is resulting from the oxidation of Mn^{II} and associated with the transformation from Mn^{III} to Mn^{IV}.[15a] The peaks at −0.948 and −0.864 V are ascribed to the redox process of W centers. The peak potential difference of this redox waves is 84 mV indicating one-electron charge-transfer processes.[15b] We also investigated the effect of the scan rates (v) on the peak currents (i_{pa} and i_{pc}) from 25 to 150 mV s^{-1} (Fig. S10 in the ESI†). The W-reduction peak and Mn-oxidation peak currents were proportional to the square root of the potential scan rate, suggesting a diffusion-controlled process[16] (Fig. S11 in the ESI†). Moreover, the stability of **1** is investigated in pH = 6 (1 M CH_3COONa/CH_3COOH) buffer with UV-vis spectra for six hours. The curves were unchanged with time (Fig. S12 in the ESI†), indicating that **1** is stable in pH 6 buffer solution.

Thermogravimetric analysis (TGA) was measured in the range of 25–600 °C under an N_2 atmosphere (Fig. S13 in the ESI†). The first weight loss was observed in the range of 25–430 °C, attributing to the removal of water molecules, and the second weight loss was observed in the range of 490–550 °C, attributing to the removal of the CO_3^{2-} ion.

Conclusions

In summary, the new trimeric, CO_3^{2-}-containing, Mn-substituted silicotungstate has been synthesized by the interaction of $[Mn_{12}O_2(OMe)_2(thme)_4(OAc)_{10}(H_2O)_4]\cdot 2MeOH$ and monolacunary $[SiW_{11}O_{39}]^{8-}$. **1** represents the first Mn-substituted silicotungstate trimer in which CO_3^{2-} resides inside the three Keggin $\{SiW_{10}Mn^{II}Mn^{III}O_{38}\}$ units with its three O atoms participating in the coordination. Even though our efforts to anchor a modified $[Mn^{II}_4Mn^{III}_4Mn^{II}_4]$ cluster onto selected lacunary POM ligand surfaces without disrupting its core structure to make the resulting compound show that SMM behavior has met with no success, we did introduce a new Mn complex as an innovative manganese source to provide Mn ions. Moreover, the synthesis of **1** provides a new route to prepare novel aggregates. Preliminary variable-temperature magnetic susceptibility measurement shows the presence of antiferromagnetic interactions in **1**. Our further research will concentrate on investigating its applications, and explore other POM ligands to react with $\{Mn_{12}\}$ to obtain a new compound containing Mn^{III} with interesting magnetic properties.

We gratefully acknowledge financial support from the National Natural Science Foundation of China, the Foundation of Education Department of Henan Province and the Natural Science Foundation of Henan Province.

Notes and references

‡ Crystal data for **1**: CSD 429047. M_r = 8881.62, hexagonal, space group $R3m$, a = 30.130(3) Å, b = 30.130(3) Å, c = 13.5343(16) Å, α = 90°, β = 90°, γ = 120°, V = 10 641(2), Z = 3, μ = 25.137 mm^{-1}, $F(000)$ = 11 607, GOF = 1.038, of 18 182 total reflections collected, 4256 were unique (R_{int} = 0.0530). R_1 (wR_2) = 0.0336 (0.0811) for 212 parameters and 4256 reflections [$I > 2\sigma(I)$].

1 (*a*) X. B. Han, Z. M. Zhang, T. Zhang, Y. G. Li, W. B. Lin, W. S. You, Z. M. Su and E. B. Wang, *J. Am. Chem. Soc.*, 2014, **136**, 5359; (*b*) A. J. Tasiopoulos, A. Vinslava, W. Wernsdorfer, K. A. Abboud and G. Christou, *Angew. Chem., Int. Ed.*, 2004, **43**, 2117; (*c*) J. Soriano-López, S. Goberna-Ferrón, L. Vigara, J. J. Carbó, J. M. Poblet and J. R. Galán-Mascarós, *Inorg. Chem.*, 2013, **52**, 4753; (*d*) R. A. Scullion, A. J. Surman, F. Xu, J. S. Mathieson, D. L. Long, F. Haso, T. B. Liu and L. Cronin, *Angew. Chem., Int. Ed.*, 2014, **53**, 10032; (*e*) J. Y. Niu, F. Li, J. W. Zhao, P. T. Ma, D. D. Zhang, B. Bassil, U. Kortz and J. P. Wang, *Chem. – Eur. J.*, 2014, **20**, 9852.

2 (*a*) Z. M. Zhang, S. Yao, Y. G. Li, H. H. Wu, Y. H. Wang, M. Rouzières, R. Clérac, Z. M. Su and E. B. Wang, *Chem. Commun.*, 2013, **49**, 2515; (*b*) J. D. Compain, P. Mialane, A. Dolbecq, I. M. Mbomekallé, J. Marrot, F. Sécheresse,

E. Rivière, G. Rogez and W. Wernsdorfer, *Angew. Chem., Int. Ed.*, 2009, **48**, 3077; (*c*) M. Ibrahim, Y. H. Lan, B. S. Bassil, Y. X. Xiang, A. Suchopar, A. K. Powell and U. Kortz, *Angew. Chem., Int. Ed.*, 2011, **50**, 4708; (*d*) C. Lydon, M. M. Sabi, M. D. Symes, D. L. Long, M. Murrie, S. Yoshii, H. Nojiri and L. Cronin, *Chem. Commun.*, 2012, **48**, 9819; (*e*) H. E. Moll, A. Dolbecq, J. Marrot, G. Rousseau, M. Haouas, F. Taulelle, G. Rogez, W. Wernsdorfer, B. Keita and P. Mialane, *Chem. – Eur. J.*, 2012, **18**, 3845.

3 (*a*) J. Thiel, P. I. Molina, M. D. Symes and L. Cronin, *Cryst. Growth Des.*, 2012, **12**, 902; (*b*) Q. Wu, Y. G. Li, Y. H. Wang, E. B. Wang, Z. M. Zhang and R. Clérac, *Inorg. Chem.*, 2009, **48**, 1606; (*c*) X. K. Fang and M. Luban, *Chem. Commun.*, 2011, **47**, 3066; (*d*) B. S. Bassil, M. Ibrahim, R. Al-Oweini, M. Asano, Z. X. Wang, J. V. Tol, N. S. Dalal, K. Y. Choi, R. N. Biboum, B. Keita, L. Nadjo and U. Kortz, *Angew. Chem., Int. Ed.*, 2011, **50**, 5961; (*e*) X. K. Fang, P. Kögerler, Y. Furukawa, M. Speldrich and M. Luban, *Angew. Chem., Int. Ed.*, 2011, **50**, 5212.

4 (*a*) C. Ritchie, A. Ferguson, H. Nojiri, H. N. Miras, Y. F. Song, D. L. Long, E. Burkholder, M. Murrie, P. Kögerler, E. K. Brechin and L. Cronin, *Angew. Chem., Int. Ed.*, 2008, **47**, 5609; (*b*) X. K. Fang, P. Kögerler, M. Speldrich, H. Schilder and M. Luban, *Chem. Commun.*, 2012, **48**, 1218; (*c*) X. K. Fang, K. McCallum, H. D. Pratt III, T. M. Anderson, K. Dennis and M. Luban, *Dalton Trans.*, 2012, **41**, 9867.

5 U. Kortz and S. Matta, *Inorg. Chem.*, 2001, **40**, 815.

6 (*a*) F. Y. Li, W. H. Guo, L. Xu, L. F. Ma and Y. C. Wang, *Dalton Trans.*, 2012, **41**, 9220; (*b*) X. K. Fang, T. M. Anderson, W. A. Neiwert and C. L. Hill, *Inorg. Chem.*, 2003, **42**, 8600.

7 N. Haraguchi, Y. Okaue, T. Isobe and Y. Matsuda, *Inorg. Chem.*, 1994, **33**, 1015.

8 Y. G. Li, W. Wernsdorfer, R. Clérac, I. J. Hewitt, C. E. Anson and A. K. Powell, *Inorg. Chem.*, 2006, **45**, 2376.

9 (*a*) S. G. Mitchell, S. Khanra, H. N. Miras, T. Boyd, D. L. Long and L. Cronin, *Chem. Commun.*, 2009, 2712; (*b*) L. J. Chen, D. Y. Shi, J. W. Zhao, Y. L. Wang, P. T. Ma, J. P. Wang and J. Y. Niu, *Cryst. Growth Des.*, 2011, **11**, 1913.

10 R. Stomberg, *Acta Chem., Scand. Ser. A*, 1985, **39**, 507.

11 (*a*) Y. Kikukawa, K. Yamaguchi, M. Hibino and N. Mizuno, *Inorg. Chem.*, 2011, **50**, 12411; (*b*) B. Botar, Y. V. Geletii, P. Kögerler, D. G. Musaev, K. Morokuma, I. A. Weinstock and C. L. Hill, *J. Am. Chem. Soc.*, 2006, **128**, 11268.

12 (*a*) I. D. Brown and D. Altermatt, *Acta Crystallogr., Sect. B: Struct. Sci.*, 1985, **41**, 244; (*b*) H. H. Thorp, *Inorg. Chem.*, 1992, **31**, 1585.

13 I. M. Szilágyi, F. Hange, J. Madarász and G. Pokol, *Eur. J. Inorg. Chem.*, 2006, 3413.

14 (*a*) B. R. Strohmeier and D. M. Hercules, *J. Phys. Chem.*, 1984, **88**, 4922; (*b*) Y. F. Han, F. X. Chen, Z. Y. Zhong, K. Ramesh, L. W. Chen and E. Widjaja, *J. Phys. Chem. B*, 2006, **110**, 24450.

15 (*a*) B. Keita, P. Mialane, F. Sécheresse, P. de Oliveira and L. Nadjo, *Electrochem. Commun.*, 2007, **9**, 164; (*b*) J. Zhao, J. S. Wang, J. W. Zhao, P. T. Ma, J. P. Wang and J. Y. Niu, *Dalton Trans.*, 2012, **41**, 5832.

16 (*a*) S. G. Mitchell, P. I. Molina, S. Khanra, H. N. Miras, A. Prescimone, G. J. T. Cooper, R. S. Winter, E. K. Brechin, D. L. Long, R. J. Cogdell and L. Cronin, *Angew. Chem., Int. Ed.*, 2011, **50**, 9154; (*b*) R. Al-Oweini, B. S. Bassil, J. Friedl, V. Kottisch, M. Ibrahim, M. Asano, B. Keita, G. Novitchi, Y. H. Lan, A. Powell, U. Stimming and U. Kortz, *Inorg. Chem.*, 2014, **53**, 5663; (*c*) B. S. Bassil, M. Ibrahim, S. S. Mal, A. Suchopar, R. N. Biboum, B. Keita, L. Nadjo, S. Nellutla, J. V. Tol, N. S. Dalal and U. Kortz, *Inorg. Chem.*, 2010, **49**, 4949.

